

# Pion mass dependence of the electromagnetic form factors of singly heavy baryons

June-Young Kim<sup>1,2,\*</sup> and Hyun-Chul Kim<sup>2,3,†</sup>

<sup>1</sup>*Institut für Theoretische Physik II, Ruhr-Universität Bochum, D-44780 Bochum, Germany*

<sup>2</sup>*Department of Physics, Inha University, Incheon 22212, Republic of Korea*

<sup>3</sup>*School of Physics, Korea Institute for Advanced Study (KIAS), Seoul 02455, Republic of Korea*

(Dated: October 11, 2021)

We study the electromagnetic form factors of the lowest-lying singly heavy baryons with spin 1/2 within the framework of the chiral quark-soliton model, focusing on the comparison with recent lattice data. To compare the present results quantitatively with the lattice data, it is essential to treat the pion mass as a variable parameter, i.e., to employ the unphysical values of the pion mass, which are used in lattice calculations. While the results with the physical value of the pion mass fall off faster than those from the lattice calculations as the momentum transfer increases, the extrapolated results with larger pion masses get closer to the lattice data. This indicates that the pion mean-field approach describes structures of both the light and singly heavy baryons.

Keywords: Electromagnetic form factors of singly heavy baryons with spin 1/2, pion mass dependence, lattice QCD, the chiral quark-soliton model

arXiv:1912.01437v7 [hep-ph] 26 May 2021

---

\* E-mail: Jun-Young.Kim@ruhr-uni-bochum.de

† E-mail: hchkim@inha.ac.kr

## I. INTRODUCTION

It is of utmost importance to study electromagnetic (EM) properties of a baryon in understanding its structure. While the EM structures of light baryons have been investigated well over decades, those of singly heavy baryons have not been much examined. The reason is that it is rather difficult to get access to EM properties of singly heavy baryons experimentally. On the other hand, very recently, EM form factors of the singly heavy baryons [1] have been investigated in a lattice QCD, which provide essential information on the EM structure of them. In Refs. [1] large values of the unphysical pion mass were employed. When one computes observables of hadrons, it is critical to consider those values of the unphysical pion mass used in lattice calculations, so that one can compare quantitatively the results from a certain model with those from the lattice data.

References [2, 3] investigated the nucleon mass and energy-momentum tensor form factors of the nucleon, emphasizing the comparison of the results with the lattice data, based on the chiral quark-soliton model ( $\chi$ QSM). In particular, Ref. [2] showed that the  $\chi$ QSM describes remarkably well the lattice data on the nucleon mass. This  $\chi$ QSM [4] was constructed based on an idea that a baryon can be viewed as a state of  $N_c$  (the number of colors) valence quarks bound by the pion mean field. This mean-field approach is justified in the large  $N_c$  limit [5, 6], since the quantum fluctuation of the meson fields is of order  $1/N_c$ , which can be neglected in this limit. The presence of the  $N_c$  valence quarks gives rise to the vacuum polarization that produces the pion mean fields. Then the pion mean fields affect self-consistently the  $N_c$  valence quarks. This self-consistent process makes a baryon emerge as a chiral soliton, which is a bound state of the  $N_c$  valence quarks. The  $\chi$ QSM has been successfully used to explain properties of the SU(3) light baryons [7–9] (see also Ref. [10] that took a somewhat different approach). The  $\chi$ QSM was extended to a singly heavy baryon that can be regarded as a bound state of  $N_c - 1$  valence quarks in the large  $N_c$  limit [11, 12]. A heavy quark inside the singly heavy baryon can be treated as a static color source when the heavy quark mass ( $m_Q$ ) is taken to be infinitely heavy. The explicit effects of the heavy-quark mass only appear in the splitting of the baryon sextet representations that are degenerate in the limit of  $m_Q \rightarrow \infty$ . The model was successfully applied to the description of properties of the lowest-lying heavy baryons such as the mass splittings [11, 13, 14], isospin mass differences [15], magnetic and transition magnetic moments [16, 17], and radiative decays [17].

As already explained in Refs. [2, 3], an original purpose of studying the pion mass dependence within the  $\chi$ QSM is to connect the results from chiral perturbation theory ( $\chi$ Pt) and those from lattice QCD, which is often called the chiral extrapolation. The  $\chi$ QSM serves well for this purpose. Even though one takes a very large value of the pion mass, the  $\chi$ QSM provides a stable chiral soliton. When one takes a limit of the heavy pion mass, we find that a light quark tends to behave as a heavy quark. Consequently the pion mean field seems to be suppressed as the pion mass increases, which will be explicitly shown later. On the other hand, the opposite limit, i.e., the chiral limit, does not commute with the large  $N_c$  limit [18, 19]. In the  $\chi$ QSM, we adopt the following strategy: one first take the limit of  $N_c \rightarrow \infty$  while keeping  $m_\pi$  finite. Then, the  $\chi$ QSM produces properly a leading non-analytic term of the nucleon mass expanded with respect to the pion mass [20–22]. This indicates that the  $\chi$ QSM inherits a correct chiral behavior. This is natural, since the model incorporates chiral symmetry and its spontaneous breakdown.

Very recently, the electric monopole ( $E0$ ) and magnetic dipole ( $M1$ ) form factors of the lowest-lying singly heavy baryons were investigated within the framework of the  $\chi$ QSM [23]. In the present work, we extend the previous work by extrapolating the experimental value of the physical pion mass to unphysical ones that correspond to the values employed in the lattice calculations. As mentioned previously, a virtue of the  $\chi$ QSM is that it can be easily associated with a value of the unphysical pion mass that is used in any lattice calculation. Thus, in the present work, we will examine the pion mass dependence of the EM form factors of the singly heavy baryons with spin 1/2 in the context of a recent lattice work [1]. We will soon see that by incorporating the unphysical values of the pion mass the present results describes better the those from the lattice data.

The present paper is organized as follows: In Section II, we recapitulate briefly how the EM form factors of the singly heavy baryons are computed within the framework of the  $\chi$ QSM. In Section III, we present the numerical results of the form factors in comparison with the lattice data. In Section IV, we summarize the present work and draw conclusions.

## II. ELECTROMAGNETIC FORM FACTORS IN THE $\chi$ QSM

Since we have presented the formalism as to how the EM form factors of singly heavy baryons with spin 1/2 were derived in Ref. [23], we will briefly recapitulate it, emphasizing dependence of the EM form factors on the pion mass. The EM current including a heavy quark is defined by

$$J_\mu(x) = \bar{\psi}(x)\gamma_\mu\hat{Q}\psi(x) + e_Q\bar{\Psi}(x)\gamma_\mu\Psi(x), \quad (1)$$

where the first term of Eq. (1) denotes the EM current of the light quarks whereas the second one corresponds to that of the heavy quark.  $\hat{Q}$  is the charge matrix of the light quarks given by

$$\hat{Q} = \begin{pmatrix} \frac{2}{3} & 0 & 0 \\ 0 & -\frac{1}{3} & 0 \\ 0 & 0 & -\frac{1}{3} \end{pmatrix} = \frac{1}{2} \left( \lambda_3 + \frac{1}{\sqrt{3}} \lambda_8 \right), \quad (2)$$

where  $\lambda_3$  and  $\lambda_8$  designate the flavor SU(3) Gell-Mann matrices.  $e_Q$  in the second part of Eq. (1) is the corresponding charge of a heavy quark:  $e_c = 2/3$  for a charm quark or  $e_b = -1/3$  for a beauty quark. In the present pion mean-field approach, we take the limit of the infinitely heavy-quark mass ( $m_Q \rightarrow \infty$ ), so that the second part of Eq. (1) provides only the constant charge to the electric form factor of a singly heavy baryon. Since the magnetic form factor of a heavy quark is proportional to its inverse mass, i.e.,  $\boldsymbol{\mu} \sim (e_Q/m_Q)\boldsymbol{\sigma}$ , we can safely neglect the heavy-quark contribution to the magnetic form factor.

The EM form factors of the singly heavy baryons are related to the matrix element of the EM current between the singly heavy baryon states with spin 1/2 as

$$\langle B, p' | J_\mu(0) | B, p \rangle = \bar{u}_B(p', \lambda') \left[ \gamma_\mu F_1(q^2) + i\sigma_{\mu\nu} \frac{q^\nu}{2M_B} F_2(q^2) \right] u_B(p, \lambda), \quad (3)$$

where  $q^2$  denotes the square of the four-momentum transfer  $q^2 = -Q^2$  with  $Q^2 > 0$ .  $u_B(p, \lambda)$  stands for the Dirac spinor with four-momentum  $p$  and the helicity  $\lambda$  for a baryon  $B$  with spin 1/2. The EM Sachs form factors  $G_E(Q^2)$  and  $G_M(Q^2)$  can be expressed in terms of the Dirac and Pauli form factors  $F_1(Q^2)$  and  $F_2(Q^2)$

$$\begin{aligned} G_E^B(Q^2) &= F_1^B(Q^2) - \tau F_2^B(Q^2), \\ G_M^B(Q^2) &= F_1^B(Q^2) + F_2^B(Q^2), \end{aligned} \quad (4)$$

with  $\tau = Q^2/4M_B^2$ . In the Breit frame, the matrix elements for the temporal and spatial components of the EM current give the electric and magnetic form factors, respectively.

$$\begin{aligned} \langle B, p' | J_0(0) | B, p \rangle &= G_E^B(Q^2) \delta_{\lambda'\lambda}, \\ \langle B, p' | J^k(0) | B, p \rangle &= \frac{i}{2M_B} (\boldsymbol{\sigma} \times \mathbf{q})^k_{\lambda'\lambda} G_M^B(Q^2), \end{aligned} \quad (5)$$

where the subscripts  $\lambda'$  and  $\lambda$  indicate the matrix elements in the two-component helicity basis. Thus, we can evaluate the EM form factors of the singly heavy baryons by computing the matrix elements of the EM current within the framework of the  $\chi$ QSM.

The  $\chi$ QSM is described by the low-energy effective QCD partition function in Euclidean space

$$\mathcal{Z}_{\chi\text{QSM}} = \int \mathcal{D}U \exp(-S_{\text{eff}}), \quad (6)$$

where the quark fields have been integrated out.  $S_{\text{eff}}$  denotes the effective chiral action

$$S_{\text{eff}}[U] = -N_c \text{Tr} \ln(i\not{D} + iMU^{\gamma_5} + i\hat{m}), \quad (7)$$

with the number of colors,  $N_c$ . Here,  $M$  stands for the dynamical quark mass that is the only free parameter of the model. We will discuss later the procedure of fixing parameters including  $M$ .  $U^{\gamma_5}$  represents the chiral field

$$U^{\gamma_5} = \exp(i\pi^a \lambda^a \gamma_5) = \frac{1 + \gamma_5}{2} U + \frac{1 - \gamma_5}{2} U^\dagger, \quad (8)$$

with  $U = \exp(i\pi^a \lambda^a)$ .  $\pi^a$  designates the pseudo-Nambu-Goldstone fields with the flavor index  $a$  running over  $a = 1, \dots, 8$ .  $\hat{m}$  is the matrix of the current-quark masses  $\hat{m} = \text{diag}(m_u, m_d, m_s)$ . We will assume isospin symmetry in the present work, so that  $m_u = m_d$ . The average mass of the up and down quarks will be defined by  $m_0 = (m_u + m_d)/2$ . The effective chiral action can be expressed in terms of the Dirac one-body Hamiltonian  $h(U)$

$$S_{\text{eff}} = -N_c \text{Tr} \ln (\partial_4 + h(U) + \gamma_4 \hat{m} - \gamma_4 m_0 \mathbf{1}), \quad (9)$$

where  $h(U)$  is written by

$$h(U) = -i\gamma_4 \gamma_i \partial_i + \gamma_4 M U + \gamma_4 m_0 \mathbf{1}. \quad (10)$$

We introduce a new mass matrix for the current quarks

$$\delta m = \hat{m} - m_0 \mathbf{1} = \frac{-m_0 + m_s}{3} \mathbf{1} + \frac{m_0 - m_s}{\sqrt{3}} \lambda^8 = m_1 \mathbf{1} + m_8 \lambda^8, \quad (11)$$

where  $m_1$  and  $m_8$  are respectively defined by

$$m_1 = \frac{1}{3}(-m_0 + m_s), \quad m_8 = \frac{1}{\sqrt{3}}(m_0 - m_s). \quad (12)$$

The integral over the  $U$  field can be performed by the saddle-point approximation that is justified in the large  $N_c$  limit. Since we have to preserve the hedgehog symmetry given by

$$\pi^a = n^a P(r), \quad \pi^b = 0 \text{ with } b = 4, \dots, 8 \quad (13)$$

with the profile function  $P(r)$  of the classical soliton, we need to embed the  $SU(2)$   $U_0$  field into  $SU(3)$  [6]

$$U = \begin{pmatrix} U_0 & 0 \\ 0 & 1 \end{pmatrix}, \quad (14)$$

where  $U_0$  denotes the  $SU(2)$  chiral field

$$U_0 = \exp[in^a \tau^a P(r)]. \quad (15)$$

As shown explicitly in Ref. [13, 14], the classical mass of a singly heavy baryon can be derived by computing the baryon correlation function in large Euclidean time. Then, the classical soliton mass is obtained to be the sum of the energies of the valence and sea quarks,  $M_{\text{sol}} = (N_c - 1)E_{\text{val}} + E_{\text{sea}}$ . Then, the classical equation of motion can be derived by minimizing the energy of the classical soliton

$$\frac{\delta}{\delta P(r)} [(N_c - 1)E_{\text{val}} + E_{\text{sea}}] \Big|_{P_c} = 0, \quad (16)$$

where  $P_c$  is the profile function of the soliton at the stationary point, which is just a solution of the pion mean fields. Hence, the soliton mass for the singly heavy baryon is finally obtained as

$$M_{\text{sol}} = (N_c - 1)E_{\text{val}}(P_c) + E_{\text{sea}}(P_c). \quad (17)$$

The classical mass  $M_{\text{cl}}$  is defined as

$$M_{\text{cl}} = M_{\text{sol}} + m_Q, \quad (18)$$

where  $m_Q$  is the effective heavy quark mass which includes the binding energy of the heavy quark.

Since we are interested in computing the EM form factors of the singly heavy baryons with the pion mass varied, we have to derive the profile function, given a value of the unphysical pion mass (see Appendix A for details as to how we can fix the parameters in the mesonic sector). Consequently, the soliton mass for the singly heavy baryon depends on the pion mass. If the value of the pion mass or that of  $m_0$  grows, the soliton mass will converge on  $2m_0$ , i.e.,

$$\lim_{m_0 \rightarrow \infty} M_{\text{sol}}(m_0) = (N_c - 1)m_0, \quad (19)$$

which was already shown in Ref. [2]. We will call it the relation for the soliton mass in the limit of large light quark mass. In Fig. 1 we draw the soliton mass as a function of  $m_0$ . The result indicates that the soliton mass converges on  $2m_0$  as  $m_0$  increases. The numerical result indeed satisfies Eq. (19). It means that as  $m_0$  increases, the effects of the pion mean field are relatively reduced.

The general formalism for the EM form factors of the singly heavy baryons with spin 1/2 was already given in Ref. [23] in detail. Thus, we will only compile the final expressions in the following:

$$G_E^B(q^2) = \int d^3z j_0(|\mathbf{q}||\mathbf{z}|) \mathcal{G}_E^B(\mathbf{z}) + G_E^Q(q^2), \quad (20)$$

$$G_M^B(q^2) = \frac{M_B}{|\mathbf{q}|} \int d^3z \frac{j_1(|\mathbf{q}||\mathbf{z}|)}{|\mathbf{z}|} \mathcal{G}_M^B(\mathbf{z}), \quad (21)$$

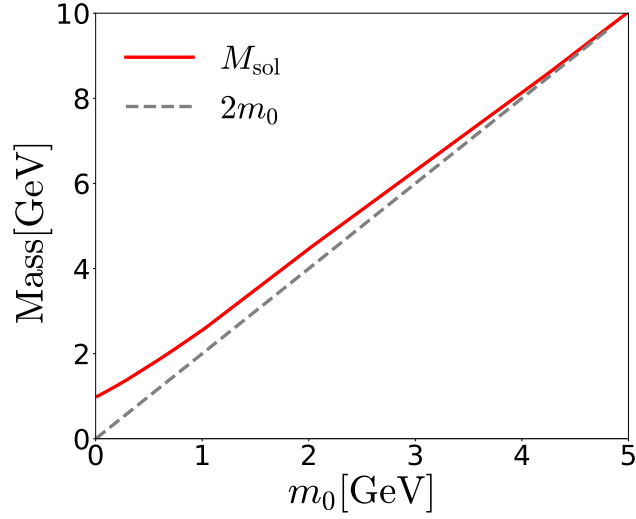


FIG. 1. Dependence of the soliton mass on  $m_0$ . The solid curve draws the result for the soliton mass as the  $m_0$  varied. the dashed one depicts  $2m_0$ .

where

$$\begin{aligned}
\mathcal{G}_E^B(\mathbf{z}) = & \frac{1}{\sqrt{3}} \langle D_{Q8}^{(8)} \rangle_B \mathcal{B}(\mathbf{z}) - \frac{2}{I_1} \langle D_{Qi}^{(8)} \hat{J}_i \rangle_B \mathcal{I}_1(\mathbf{z}) - \frac{2}{I_2} \langle D_{Qp}^{(8)} \hat{J}_p \rangle_B \mathcal{I}_2(\mathbf{z}) \\
& - \frac{4m_8}{I_1} \langle D_{8i}^{(8)} D_{Qi}^{(8)} \rangle_B (I_1 \mathcal{K}_1(\mathbf{z}) - K_1 \mathcal{I}_1(\mathbf{z})) - \frac{4m_8}{I_2} \langle D_{8p}^{(8)} D_{Qp}^{(8)} \rangle_B (I_2 \mathcal{K}_2(\mathbf{z}) - K_2 \mathcal{I}_2(\mathbf{z})) \\
& - 2 \left( \frac{m_1}{\sqrt{3}} \langle D_{Q8}^{(8)} \rangle_B + \frac{m_8}{3} \langle D_{88}^{(8)} D_{Q8}^{(8)} \rangle_B \right) \mathcal{C}(\mathbf{z}), \tag{22}
\end{aligned}$$

$$\begin{aligned}
\mathcal{G}_M^B(\mathbf{z}) = & \langle D_{Q3}^{(8)} \rangle_B \left( \mathcal{Q}_0(\mathbf{z}) + \frac{1}{I_1} \mathcal{Q}_1(\mathbf{z}) \right) - \frac{1}{\sqrt{3}} \langle D_{Q8}^{(8)} \hat{J}_3 \rangle_B \frac{1}{I_1} \mathcal{X}_1(\mathbf{z}) - \langle d_{pq3} D_{Qp}^{(8)} \hat{J}_q \rangle_B \frac{1}{I_2} \mathcal{X}_2(\mathbf{z}) \\
& + \frac{2}{\sqrt{3}} m_8 \langle D_{83}^{(8)} D_{Q8}^{(8)} \rangle_B \left( \frac{K_1}{I_1} \mathcal{X}_1(\mathbf{z}) - \mathcal{M}_1(\mathbf{z}) \right) + 2m_8 \langle d_{pq3} D_{8p}^{(8)} D_{Qq}^{(8)} \rangle_B \left( \frac{K_2}{I_2} \mathcal{X}_2(\mathbf{z}) - \mathcal{M}_2(\mathbf{z}) \right) \\
& - 2 \left( m_1 \langle D_{Q3}^{(8)} \rangle_B + \frac{1}{\sqrt{3}} m_8 \langle D_{88}^{(8)} D_{Q3}^{(8)} \rangle_B \right) \mathcal{M}_0(\mathbf{z}). \tag{23}
\end{aligned}$$

The explicit expressions for those densities, and moments of inertia  $I_{1,2}$  and  $K_{1,2}$  are given already in Ref. [23].  $G_E^Q(q^2)$  in Eq. (21) represents the heavy-quark contribution to an electric form factor of a singly heavy baryon. In the limit of  $m_Q \rightarrow \infty$ , it gives just the charge of the corresponding heavy quark.

### III. RESULTS AND DISCUSSION

Before we present the numerical results, we first explain briefly how to determine the model parameters. We fix them first in the mesonic sector. Since the pion decay constant diverges logarithmically, which arises from the corresponding quark loop, we need to introduce a regularization scheme. In the present work, we adopt the proper-time regularization with the cutoff mass  $\Lambda$  that can be fixed by reproducing the experimental value of the pion decay constant  $f_\pi = 93$  MeV. The average value of the up and down current quark masses,  $m_0$ , is determined by reproducing the physical value of the pion mass  $m_\pi = 140$  MeV. The only free parameter is then the dynamical quark mass,  $M$ , which will be determined by reproducing various properties of the proton. The best value turns out to be  $M = 420$  MeV and we keep using this value also for the heavy baryon sector.

Since we want to extrapolate the present model by employing various different values of the unphysical pion mass, we have to proceed to fix the parameters very carefully. As we explain in Appendix A in detail, one should distinguish  $M$  from  $M' = M + m_0$  that appears in the expressions for the quark condensate and pion decay constant. The value of the dynamical quark mass  $M$  is always fixed to be 420 MeV. We want to mention that there is one caveat related

to the pion decay constant. In effect, the value of the pion decay constant increases as that of the unphysical pion mass increases in lattice calculations. However, since the pion decay constant is divergent logarithmically, its change is rather mild as the pion mass varies. Indeed, the value of the pion decay constant from the lattice QCD [24, 25] is enhanced by about 30 % when the value of  $m_\pi$  is taken to be approximately 0.5 GeV. This means that it is still approximately valid to keep using the experimental value of the pion decay constant to fix the cutoff mass  $\Lambda$ . Thus, we will continue to use it to fix the cutoff mass as our prescription. On the other hand, the average mass of the up and down valence quarks  $m_0$  depends directly on the value of the unphysical pion mass, which we have to consider seriously.

This strategy for comparison with the lattice results was already discussed in Ref. [2] in detail. Of course we could have taken the values of  $f_\pi(m_\pi)$  produced in lattice calculations as input. This means that both the pion decay constant and the quark condensate securely increase as  $m_\pi$  increases. In this case, the results for the EM form factors of singly heavy baryons are obtained to be almost the same as the present ones. However, there is a caveat in this analysis. If one increases the pion mass larger than 400 MeV, then the soliton solution does not exist. This is no wonder: the parameters  $f_\pi$ ,  $m_\pi$ ,  $m_0$ , and  $\Lambda$  in the present model are interrelated, so that we are not able to change one of them independently while keeping the soliton solution stable. Thus, we will rather regard the discrepancy for the pion decay constant arising from the comparison with the lattice results as the model accuracy, since the present model is used to describe the observables within the (5 – 30) % accuracy.

Given a value of the unphysical pion mass, then we are able to fix  $\Lambda$  for regulators and the current quark mass  $m_0$  by using Eq. (A2) and Eq. (A4). From those fixed parameters, we get the chiral condensate, also known as the chiral order parameter,  $\langle\bar{\psi}\psi\rangle$  defined in Eq. (A1). It characterizes the strength of the spontaneous breakdown of chiral symmetry. As shown in Eq. (A1), it is inevitable to provide the numerical value of  $M$  to determine the quark condensate. The same is true also for the pion decay constant (see Eq. (A2)). Another physical implication of the dynamical quark mass is the coupling strength between the quark and pNG fields. The strange current quark mass is taken to be  $m_s = 180$  MeV to reproduce the mass splitting of flavor SU(3) light baryons [26] and singly heavy baryons [13].

Now, a natural question may arise. Is the dynamics of the  $\chi$ QSM appropriate for extrapolating the pion mass to the unphysical ones? We can answer this question as follows: Firstly, the effective chiral action given in Eq. (7) can be derived from the QCD instanton vacuum [9, 27], which may be considered as a low-energy effective model of QCD. Actually, the dynamical quark mass from the instanton vacuum depends on the quark momentum. This momentum-dependent quark mass also plays a role of a regulator. However, we turn off the momentum dependence of the dynamical quark mass to avoid theoretical complexities and introduce an explicit regularization scheme to tame the divergences arising from the quark loops. Secondly, since the effective chiral action complies with chiral symmetry and its spontaneous breakdown, it naturally contains all orders of the effective chiral Lagrangians in the leading order of  $N_c$ . This can be shown explicitly by the derivative expansion [4, 28, 29]. Thus, the  $\chi$ QSM respects at least important symmetries and properties of low-energy QCD, so that it is in a proper position to be confronted with lattice QCD.

TABLE I. Dependence of the valence- and sea-quark energies, and the soliton mass on the values of the pion mass.

$m_\pi$ [MeV]	$m_0$ [MeV]	$\Lambda$ [MeV]	$-\langle\bar{\psi}\psi\rangle^{-1/3}$ [MeV]	$E_{\text{val}}$ [MeV]	$E_{\text{sea}}$ [MeV]	$M_{\text{sol}}$ [MeV]
140	18	637	210	645	354	999
300	75	645	206	717	362	1078
410	130	659	205	786	366	1152
570	219	689	204	908	370	1278
700	295	718	204	1019	371	1380

In Table. I, we list the numerical values of the valence- and sea-quark energies, and the soliton mass. As the pion mass increases, both the valence- and sea-quark energies increase. In consequence, the soliton mass also grows larger as a function of  $m_\pi$ . As discussed in Ref. [22], these results for the nucleon mass as a function of  $m_\pi^2$  are in good agreement with the lattice data.

We now examine the dependence of the masses of  $\Sigma_c$  and  $\Omega_c$  on the pion mass, which belong to the baryon sextet with spin 1/2, comparing the present results with those from lattice QCD. In the left panel of Fig. 2, we show the numerical results for the classical mass  $M_{\text{cl}}$  as a function of  $m_\pi^2$ . Note that for comparison with the lattice data we normalize the classical mass by the lattice value of the  $\Sigma_c$  mass at the physical value of the pion mass,  $m_\pi = 140$  MeV. Interestingly, the result of the classical mass is in very good agreement with the lattice data. In fact, the nucleon mass from the  $\chi$ QSM was shown to be almost the same as the lattice data as described in Ref. [2]. We want to

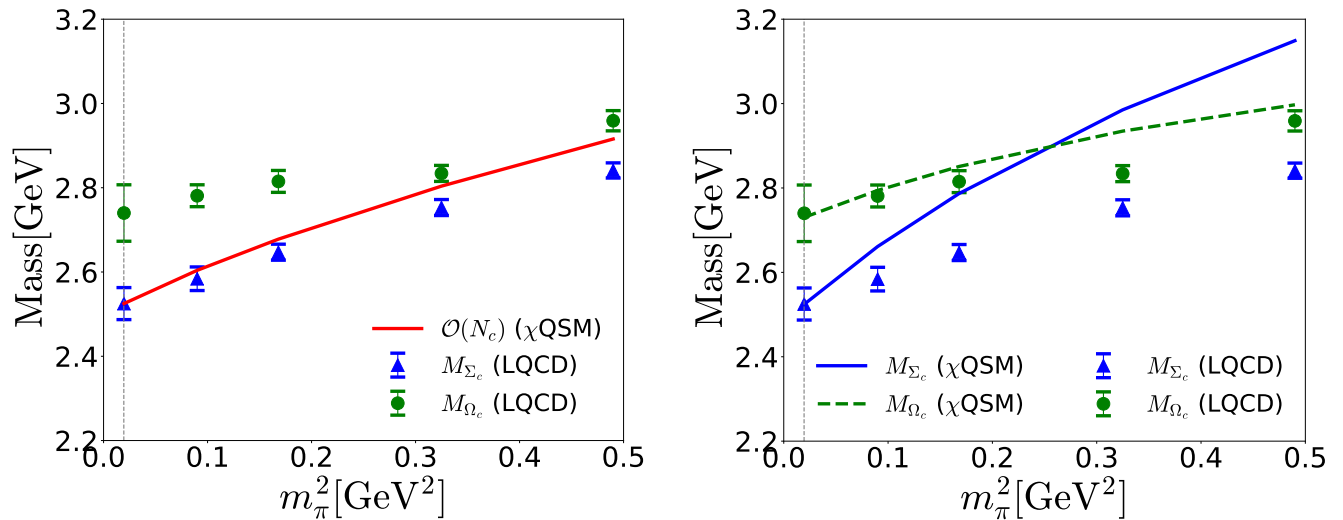


FIG. 2. Dependence of the masses of the singly heavy baryons,  $\Sigma_c$  and  $\Omega_c$ . In the left panel, we draw the classical mass as a function of  $m_\pi^2$  whereas in the right panel, we depict the masses of  $\Sigma_c$  and  $\Omega_c$  as functions of  $m_\pi^2$  in the solid and dashed curves, respectively. To compare these results with the lattice data, we normalize the classical mass by the lattice value of  $M_{\Sigma_c}$  at the physical pion mass, which is drawn as the vertical short dashed line. The lattice data are taken from Ref. [1].

mention that in Ref. [2], the nucleon mass was in fact the classical mass. As mentioned in Introduction, the chiral limit ( $m_\pi \rightarrow 0$ ) does not commute with the large  $N_c$  limit. In the  $\chi$ QSM, the strategy is that one first take the limit of  $N_c \rightarrow \infty$  while keeping  $m_\pi$  finite. Next, we take the chiral limit. In this case, the leading non-analytic term of the nucleon mass, which appears when the nucleon mass is expanded with respect to the pion mass, is yielded to be

$$M_N(m_\pi)^{\mathcal{O}(m_\pi^3)} = k \frac{3g_A^2}{32\pi f_\pi^2} m_\pi^3. \quad (24)$$

This expression reproduces that obtained in one-loop  $\chi$ PT except for the overall factor  $k$ . Chiral solitonic models give  $k = 3$  whereas  $\chi$ PT provides  $k = 1$  [30]. Here,  $g_A$  denotes the axial charge of the nucleon. This has a very important physical implication. In chiral solitonic models, the masses of the  $\Delta$  isobar and the nucleon become degenerate in the large  $N_c$  limit. Moreover, taking the large  $N_c$  limit with  $m_\pi$  kept finite, we find that  $M_\Delta - M_N$  turns out to be much smaller than the pion mass. This means that the  $\Delta$  isobar must be considered as an intermediate state in chiral loops, which provides as twice as the nucleon contribution because of the different Clebsch-Gordan coefficients, so we have  $k = 3$  [20]. In contrast, one-loop conventional  $\chi$ PT [30] takes the opposite ordering, which means that the chiral limit is taken first and then the large  $N_c$  limit is considered in  $\chi$ PT. This indicates that the mass difference  $M_\Delta - M_N$  is much larger than  $m_\pi$ . So, the contribution of the  $\Delta$  isobar in the chiral loops is ignored, which brings about the different value of  $k$ . As discussed in Ref. [20], the ratio  $d = (M_\Delta - M_N)/m_\pi$  becomes infinity in conventional  $\chi$ PT whereas it goes to zero in chiral solitonic approaches. However, the truth lies between these two values.

Based on this argument, we can consider the degenerate masses of the baryon sextet in the large  $N_c$  limit. Hence, the left panel of Fig. 2 describes the representative mass of the low-lying singly heavy baryons. In this sense, the result shown in Fig. 2 is indeed remarkable, since it describes both the lattice data on the  $\Sigma_c$  and  $\Omega_c$  masses. Thus, the  $\chi$ QSM provides a reliable framework for comparison of any observables for the singly heavy baryons with the corresponding lattice data. In the right panel of Fig. 2, we take a more realistic position. So, we introduce the rotational  $1/N_c$  and linear  $m_s$  corrections, which also depend on the pion mass. While the present result for the  $\Sigma_c$  mass, which is depicted in the solid curve, rises faster than the lattice data, that for the  $\Omega_c$  mass, drawn in the dashed curve, is in good agreement with the lattice data. In fact, the mass spectra of the low-lying singly heavy baryons were studied in Ref. [13]. The masses of the  $\Sigma_c$  and  $\Omega_c$  are expressed as

$$M_{\Sigma_c} = M_{\mathbf{6}} + \frac{2}{3}\delta_{\mathbf{6}}, \quad M_{\Omega_c} = M_{\mathbf{6}} - \frac{4}{3}\delta_{\mathbf{6}}, \quad (25)$$

where definitions of the parameters  $M_{\mathbf{6}}$  and  $\delta_{\mathbf{6}}$  can be found in Ref. [13]. The parameter  $\delta_{\mathbf{6}}$  is related to the linear ( $m_s - m_0$ ) corrections, so that it gives rise to the mass splitting in the baryon sextet. Note that  $\delta_{\mathbf{6}}$  has a negative value in the range of  $0 \leq m_\pi^2 \leq 0.25 \text{ GeV}^2$ . Then, it is changed to positive. This explains why the mass of  $\Sigma_c$  is raised faster than that of  $\Omega_c$  as shown in the right panel of Fig. 2. Note that the masses of  $\Sigma_c$  and  $\Omega_c$  coincide with each

other at around  $m_\pi^2 = 0.25 \text{ GeV}^2$ , where the average mass of the up and down current quarks turns out to be the same as that of the strange current quark. So, flavor SU(3) symmetry is restored at this point.

As mentioned previously, to examine the pion mass dependence of the EM form factors, we first have to compute the profile functions of the chiral soliton given a value of the pion mass. To do that, we choose its five different values:  $m_\pi = 140 \text{ MeV}$  (physical one),  $m_\pi = 300 \text{ MeV}$ ,  $m_\pi = 410 \text{ MeV}$ ,  $m_\pi = 570 \text{ MeV}$ , and  $m_\pi = 700 \text{ MeV}$  and derive the new profile functions corresponding to these values of the pion mass. Except for the physical one, all the values were employed by the lattice calculation [1]. So far, there is no experimental data on the EM form factors of the singly heavy baryons. Thus, in the present work, we will carefully compare the present results with those from a recent lattice work [1], considering the pion mass as a variable parameter.

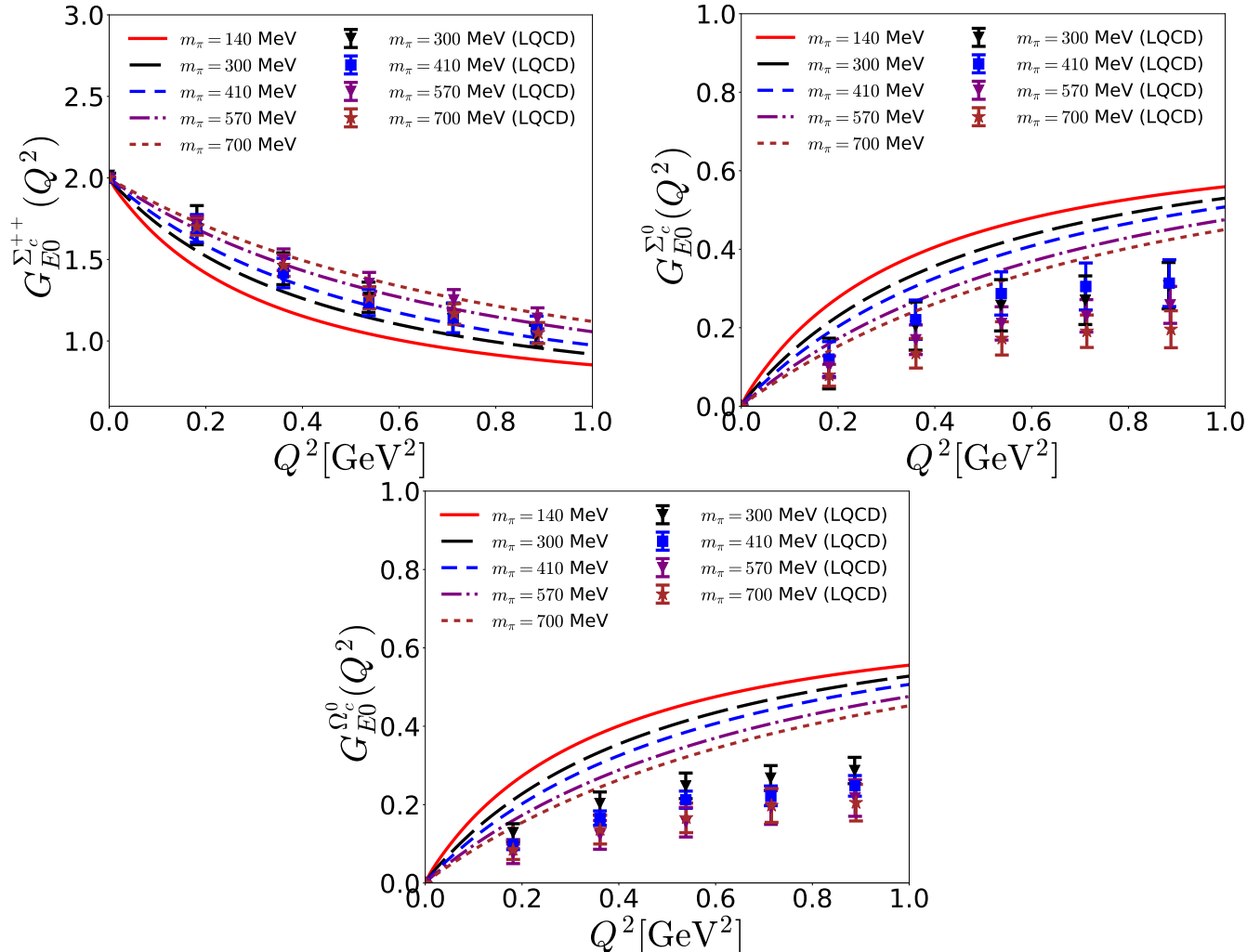


FIG. 3. Electric monopole form factors of the baryon sextet with spin-1/2 in comparison with the data from the lattice QCD. The data of the lattice QCD are taken from Ref. [1]. Note that the lattice data for the zero-charged electric form factors of the heavy baryons are taken from the private communication with U. Can [31].

We first compare the results of the  $E0$  form factors obtained from the present model with those from the lattice calculations [1], though a part of the work with the physical pion mass was already done in Ref. [23]. In Fig. 3 we draw the electric form factors of the  $\Sigma_c^{++}$ ,  $\Sigma_c^0$ , and  $\Omega_c^0$  baryons with spin 1/2 in comparison with the corresponding lattice data. we extrapolate the physical pion mass  $m_\pi = 140 \text{ MeV}$  to the unphysical ones of which the values are taken from those used in the lattice calculation, i.e. four different values  $m_\pi = 300 \text{ MeV}$ ,  $410 \text{ MeV}$ ,  $570 \text{ MeV}$ , and  $700 \text{ MeV}$ . As expected, when we increase the values of the pion mass, the results of the electric form factors fall off more slowly as  $Q^2$  increases. This is a well-known feature of the lattice results. Thus, when one wants to compare results of any form factors with those from lattice works, it is better to employ larger pion masses that match the corresponding values used in the lattice calculation. When the pion mass gets larger, the  $Q^2$  dependences of the electric form factors of the neutral heavy baryons increase more slowly. This can be understood by examining the behavior of the soliton profile

function. As the pion mass increases larger than 140 MeV, the Yukawa tail of the soliton falls off faster than this physical case. This indicates that the size of the baryon becomes more compact than the physical one. Consequently, the results for the electric form factors fall off more slowly. The numerical results for the  $\Sigma_c^{++}$  electric form factor are in agreement with the lattice data. Those for  $\Sigma_c^0$  and  $\Omega_c^0$  get closer to the data as the pion mass increases.

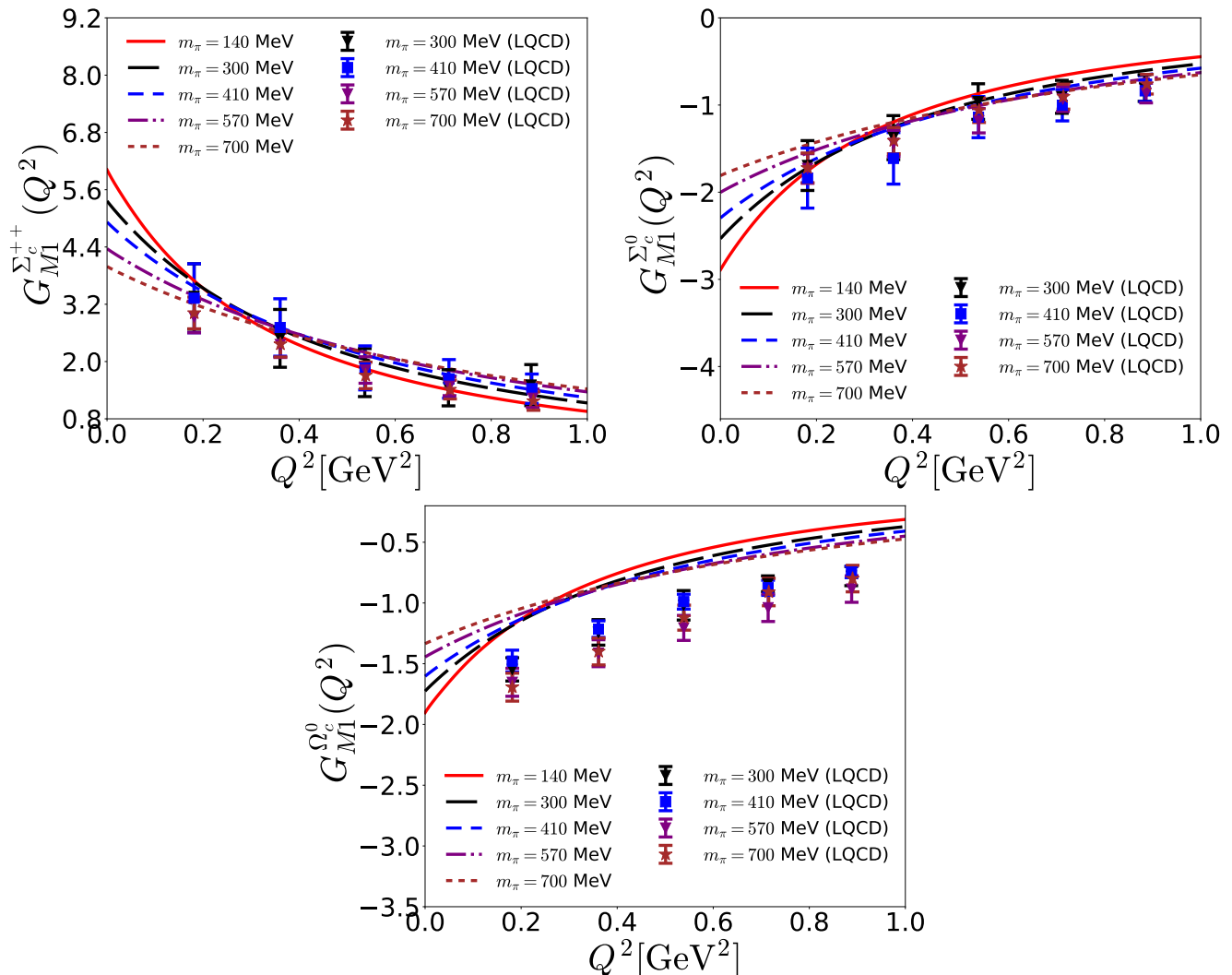


FIG. 4. Magnetic dipole form factors of the baryon sextet with spin 1/2 in comparison with the data from the lattice QCD. The data of the lattice QCD are taken from Ref. [1].

Figure 4 depicts the comparison of the present results for the  $M1$  form factors of the  $\Sigma_c^{++}$ ,  $\Sigma_c^0$ , and  $\Omega_c^0$  heavy baryons with the corresponding lattice data. Note that in order to compare the  $Q^2$  dependence, we have normalized the magnitudes of the magnetic form factors at  $Q^2 = 0$  to be the same as the lattice ones. In Ref. [1], the chiral extrapolation to the physical mass of the pion was performed. Here, we take the values of the quadratic fitting obtained from Ref. [1]: 4.12 for  $\Sigma_c^{++}$ , 3.80 for  $\Sigma_c^0$ , and 2.71 for  $\Omega_c$ . The present results on the  $Q^2$  dependence of the  $M1$  form factors are generally in qualitative agreement with the lattice data. Again we find that the lattice results fall off more slowly, compared to the present ones. In particular, the numerical results for the  $\Sigma_c^{++}$  and  $\Sigma_c^0$  magnetic form factors get closer to the lattice data as  $m_\pi$  increases. That for  $\Omega_c^0$  is also in line with the data.

Figure 5 illustrates the results for the EM form factors of the singly heavy baryons with spin 1/2 as functions of the pion mass, with  $Q^2$  fixed to be  $0.54 \text{ GeV}^2$ . The numerical results for the  $\Sigma_c^{++}$  electric and magnetic form factors are in agreement with the lattice data, as shown in the upper panel of Fig. 5. As for the EM form factors of the other heavy baryons, the present results exhibit similar dependence on the pion mass, compared with the lattice data.

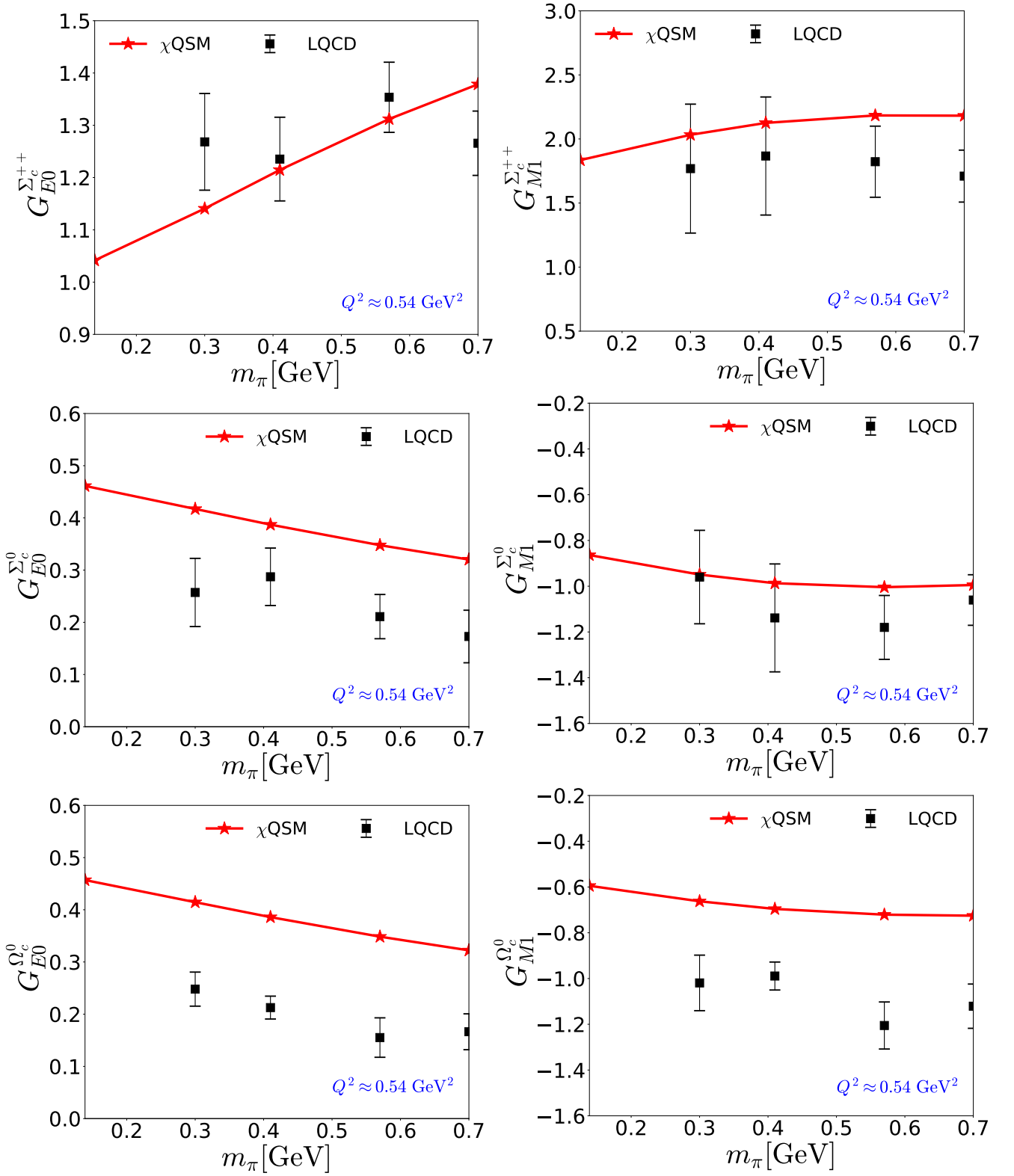


FIG. 5. Electromagnetic form factors as a function of the pion mass with the momentum transfer squared  $Q^2 \approx 0.54 \text{ GeV}^2$  fixed. The data of lattice QCD are taken from Ref. [1].

#### IV. SUMMARY AND CONCLUSION

In the present work, we have aimed at investigating the electromagnetic form factors of the lowest-lying singly heavy baryons with spin 1/2 within the framework of the chiral quark-soliton model, focusing on the comparison of the results with recent lattice data. We first derived the profile functions of the chiral soliton, employing the unphysical values of the pion mass. We examined the limit of the heavy quark mass and showed that the soliton mass consisting of the  $N_c - 1$  valence quarks converges on  $2m_0$ . This implies that the pion mean fields get relatively suppressed as the pion mass increases. Before we proceeded to compute the electromagnetic form factors, we scrutinized the classical and physical masses of the singly heavy baryons as the pion mass was varied from  $m_\pi^2 = 0.02 \text{ GeV}^2$  to  $0.5 \text{ GeV}^2$ . The classical mass is in good agreement with the lattice data on the  $\Sigma_c$  and  $\Omega_c$  masses. When we considered the rotational  $1/N_c$  corrections and the effects of flavor SU(3) symmetry breaking, the present results for the  $\Omega_c$  mass are in agreement with the lattice data. On the other hand, those of the  $\Sigma_c$  mass tends to rise faster than the data. We then calculated the electric form factors of the  $\Sigma_c^{++}$ ,  $\Sigma_c^0$ , and  $\Omega_c^0$  for which there exist the lattice data. As the pion mass increases, the present results reproduce very well the lattice data on the  $\Sigma_c^{++}$  electric form factor. For neutral heavy baryons, the results get closer to the lattice data. The results for the  $\Sigma_c^{++}$  and  $\Sigma_c^0$  magnetic form factor are also in qualitative agreement with the lattice data. Those for the  $\Omega_c$  magnetic form factor show similar  $Q^2$  dependence, compared with the data. Finally, we compared the present results for the electromagnetic form factors of the  $\Sigma_c^{++}$ ,  $\Sigma_c^0$ , and  $\Omega_c^0$  as functions of the pion mass, fixing the momentum transfer squared to be  $Q^2 = 0.54 \text{ GeV}^2$ . Again, the results for the  $\Sigma_c^{++}$  and  $\Sigma_c^0$  are in qualitative agreement with the lattice data. The results for all other form factors are similar dependence on the pion mass, compared with the lattice data.

In conclusion, the present scheme describes well the electromagnetic form factors of the lowest-lying singly heavy baryons with spin 1/2, compared with those from lattice QCD. It indicates that the singly heavy baryons with spin 1/2 are indeed well explained in the pion mean-field approximation, i.e, in the chiral quark-soliton model. The  $1/m_Q$  corrections are expected to be marginal but are very interesting issues, which will be considered in the near future.

#### ACKNOWLEDGMENTS

The authors are grateful to Gh.-S. Yang for valuable discussions. They want to express the gratitude to K. U. Can for providing us with the lattice data. The present work was supported by Inha University Research Grant. J.-Y. Kim is also supported by a DAAD doctoral scholarship.

#### Appendix A: Fixing the model parameters

Using the effective chiral action given in Eq. (7), one can derive the expressions for the chiral condensate

$$\langle \bar{\psi}\psi \rangle = - \int \frac{d^4 p_E}{(2\pi)^4} \frac{8N_c M'}{p_E^2 + M'^2} \Big|_{reg} = -8N_c M' I_1, \quad (\text{A1})$$

and for the pion decay constant

$$f_\pi^2 = - \int \frac{d^4 p_E}{(2\pi)^4} \frac{4N_c M'^2}{(p_E^2 + M'^2)^2} \Big|_{reg} = 8N_c M'^2 I_2, \quad (\text{A2})$$

where  $M' = M + m_0$ .  $I_1$  and  $I_2$  stand for the regularization functions, which are expressed as

$$\begin{aligned} I_1 &= \int_{\Lambda^{-2}}^{\infty} \frac{du}{u^2} \frac{e^{-uM'}}{(4\pi)^2}, \\ I_2 &= \int_{\Lambda^{-2}}^{\infty} \frac{du}{2u} \frac{e^{-uM'}}{(4\pi)^2} \int_0^1 d\beta e^{u\beta(1-\beta)m_\pi^2}. \end{aligned} \quad (\text{A3})$$

The pion mass is determined by the pole position of the pion propagator that is obtained by a low-energy effective chiral theory given by Eq. (6)

$$m_\pi^2 = \frac{m}{M} \frac{I_1}{I_2}. \quad (\text{A4})$$

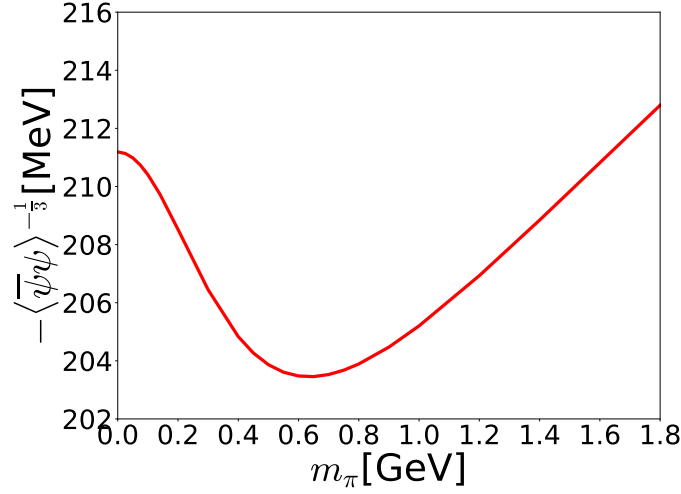


FIG. 6. Chiral condensate as a function of  $m_\pi$  with fixed  $f_\pi$  and  $M$ .

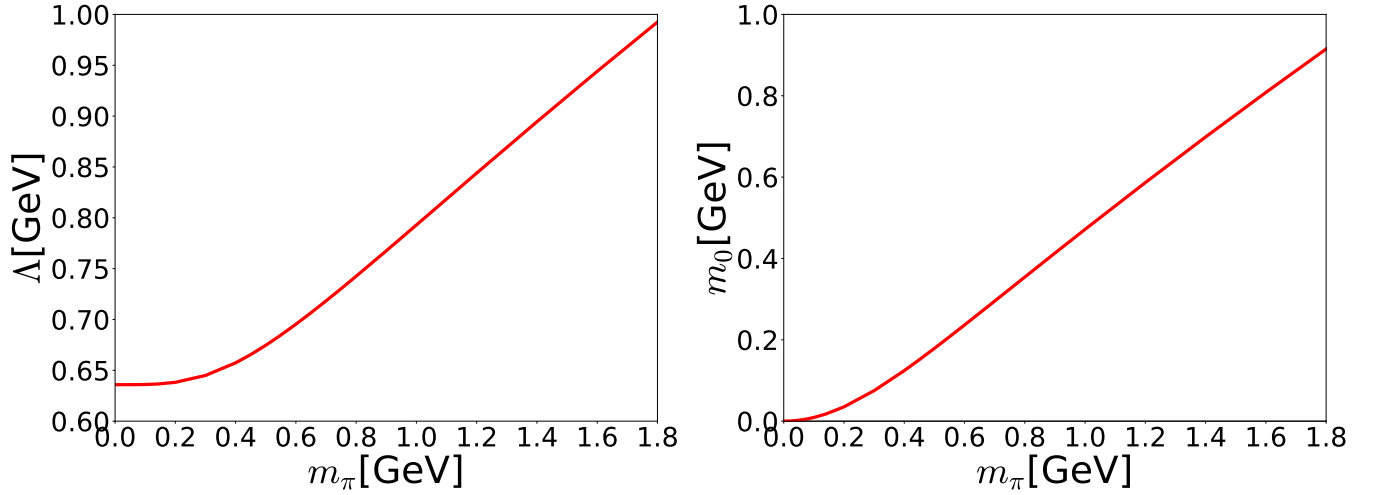


FIG. 7. Dependencies of parameters  $\Lambda$  (left panel) and  $m_0$  (right panel) on  $m_\pi$

When  $m_\pi$  is the physical one, Eq. (A2) and Eq. (A4) satisfy the Gell-Mann–Oakes–Renner(GOR) relation

$$m_\pi^2 f_\pi^2 = -m_0 \langle \bar{\psi} \psi \rangle + \mathcal{O}(m_0^2). \quad (\text{A5})$$

Using the experimental value of the pion decay constant and fixing the dynamical quark mass, we obtain the results for the current quark mass  $m_0$ , the cutoff mass  $\Lambda$  and the chiral condensate  $\langle \bar{\psi} \psi \rangle$  as functions of  $m_\pi$ . The results are drawn respectively in Fig 6 and Fig 7. In Fig. 6, we find that the results for the chiral condensate decreases till the value of  $m_\pi$  (or  $m_0$ ) reaches  $m_\pi \approx 0.6$  GeV and then increases monotonically as  $m_\pi$  further increases. Note that a lattice calculation [25] predicts monotonic increment of the chiral condensate as  $m_\pi$  increases. Thus, while the present model gives a different behavior of the chiral condensate with the lower values of  $m_\pi$ , it restores the correct behavior when  $m_\pi$  is larger than  $m_\pi \approx 0.6$  GeV. Figure 7 shows how  $\Lambda$  and  $m_0$  depend on  $m_\pi$ . Both the parameters increase as the pion mass increases.

- 
- [1] K. U. Can, G. Erkol, B. Isildak, M. Oka and T. T. Takahashi, JHEP **1405** (2014) 125 [arXiv:1310.5915 [hep-lat]].  
 [2] K. Goeke, J. Ossmann, P. Schweitzer and A. Silva, Eur. Phys. J. A **27** (2006) 77 [hep-lat/0505010].  
 [3] K. Goeke, J. Grabis, J. Ossmann, P. Schweitzer, A. Silva and D. Urbano, Phys. Rev. C **75** (2007) 055207 [hep-ph/0702031 [HEP-PH]].

- [4] D. Diakonov, V. Y. Petrov and P. V. Pobylitsa, Nucl. Phys. B **306** (1988) 809.
- [5] E. Witten, Nucl. Phys. B **160** (1979) 57.
- [6] E. Witten, Nucl. Phys. B **223** (1983) 422 and Nucl. Phys. B **223** (1983) 433.
- [7] M. Wakamatsu and H. Yoshiki, Nucl. Phys. A **524** (1991) 561.
- [8] C. V. Christov, A. Blotz, H.-Ch. Kim, P. Pobylitsa, T. Watabe, T. Meissner, E. Ruiz Arriola and K. Goeke, Prog. Part. Nucl. Phys. **37** (1996) 91 [hep-ph/9604441].
- [9] D. Diakonov, [hep-ph/9802298].
- [10] R. Alkofer, H. Reinhardt and H. Weigel, Phys. Rept. **265** (1996) 139 [hep-ph/9501213].
- [11] G. S. Yang, H.-Ch. Kim, M. V. Polyakov and M. Praszalowicz, Phys. Rev. D **94** (2016) 071502 [arXiv:1607.07089 [hep-ph]].
- [12] D. Diakonov, arXiv:1003.2157 [hep-ph].
- [13] J.-Y. Kim, H.-Ch. Kim and G. S. Yang, Phys. Rev. D **98** (2018) 054004 [arXiv:1801.09405 [hep-ph]].
- [14] J.-Y. Kim and H.-Ch. Kim, PTEP **2020** (2020) 043D03 [arXiv:1909.00123 [hep-ph]].
- [15] G. S. Yang and H.-Ch. Kim, Phys. Lett. B **808** (2020) 135619 [arXiv:2004.08524 [hep-ph]].
- [16] G. S. Yang and H.-Ch. Kim, Phys. Lett. B **781** (2018) 601 [arXiv:1802.05416 [hep-ph]].
- [17] G. S. Yang and H.-Ch. Kim, Phys. Lett. B **801** (2020) 135142 [arXiv:1909.03156 [hep-ph]].
- [18] J. Gasser, Annals Phys. **136** (1981) 62.
- [19] R. F. Dashen, E. E. Jenkins and A. V. Manohar, Phys. Rev. D **49** (1994) 4713 [arXiv:hep-ph/9310379 [hep-ph]].
- [20] T. D. Cohen and W. Broniowski, Phys. Lett. B **292** (1992) 5 [arXiv:hep-ph/9208253 [hep-ph]].
- [21] C. Schüren, E. Ruiz-Arriola and K. Goeke, Nucl. Phys. A **547** (1992) 612.
- [22] P. Schweitzer, Phys. Rev. D **69** (2004), 034003 [arXiv:hep-ph/0307336 [hep-ph]].
- [23] J.-Y. Kim and H.-Ch. Kim, Phys. Rev. D **97** (2018) 114009 [arXiv:1803.04069 [hep-ph]].
- [24] J. Noaki *et al.* [JLQCD and TWQCD], Phys. Rev. Lett. **101** (2008) 202004 doi:10.1103/PhysRevLett.101.202004 [arXiv:0806.0894 [hep-lat]].
- [25] S. Dürr *et al.* [Budapest-Marseille-Wuppertal], Phys. Rev. D **90** (2014) 114504 doi:10.1103/PhysRevD.90.114504 [arXiv:1310.3626 [hep-lat]].
- [26] A. Blotz, D. Diakonov, K. Goeke, N. W. Park, V. Petrov and P. V. Pobylitsa, Nucl. Phys. A **555** (1993) 765
- [27] D. Diakonov and V. Y. Petrov, Nucl. Phys. B **272** (1986) 457.
- [28] E. Ruiz-Arriola, Phys. Lett. B **253** (1991) 430.
- [29] H. A. Choi and H.-Ch. Kim, Phys. Rev. D **69** (2004) 054004 [arXiv:hep-ph/0308171 [hep-ph]].
- [30] E. E. Jenkins and A. V. Manohar, Phys. Lett. B **255** (1991) 558.
- [31] A private communication with U. Can (2019).